Comparative Investigation of Different Configurations of Graphene-Based Superficial Microwave Hyperthermia

alka Singla (alka.singla274@gmail.com)
SLIET: Sant Longowal Institute of Engineering and Technology https://orcid.org/0000-0001-8661-9346
Anupma Marwaha
SLIET: Sant Longowal Institute of Engineering and Technology
Sanjay Marwaha
SLIET: Sant Longowal Institute of Engineering and Technology
Murthy Chavali
NTRC: National Transport Research Centre

Original Research

Keywords: Graphene Nanomaterial, Microwave Hyperthermia, Patch applicator, Finite Element Mesh

Posted Date: February 15th, 2021

DOI: https://doi.org/10.21203/rs.3.rs-190756/v1

Abstract

For treating superficial tumours patch antennas present a more compact structure and are easy to design. Graphene-based antenna applicators can further provide an effective solution for the non-invasive procedure by selecting different configurations of the patch for producing homogeneous energy deposition. Graphene patch facilitates the reduction of surface waves among the healthy tissues. Four different antenna shapes of graphene-based antenna applicators are designed at operating frequency of 915 MHz in ISM band and comparison is performed in terms of SAR and temperature distribution. Among all the applicators triangular patch applicator outperforms in terms of more localized heating and attains the highest value of temperature at 324°K and SAR of 186 W/Kg at insertion depth of 6 mm. The double slot applicator also provides localized SAR and uniform heating but results in the lower temperature of 315°K and much reduced SAR of 41 W/Kg at same insertion depth. Further, the effect of distance between the source and tissue model has also been investigated. It has been found that SAR decreases with increased distance from the radiating source. At the optimized distance of 3 mm, SAR values obtained for rectangular, circular, triangular and double slot patch applicator are 60 W/Kg, 54.7 W/Kg, 134.1 W/Kg and 54.2 W/Kg respectively.

1. Introduction

The application of microwave energy in hyperthermia for treating cancer patients is an emerging field in the area of medical applications. The microwave energy is induced in the cancerous tissues by elevating the temperature up to 45 °C. Heat can be generated in the damaged tissues by transferring the electromagnetic energy into biological systems and electric field intensity is responsible for producing heat in tissue [1]. The wave is propagated either invasively or non-invasively in order to couple electromagnetic energy through human phantom for microwave hyperthermia treatment [2].

Various non-invasive microwave applicators such as capacitive [3], inductive [4] and waveguide applicators [5] for radio frequencies and radiative aperture applicator [6], multi-applicator, phased array [7] and microstrip antenna applicator [8] for microwave frequencies have been reported in the literature. The appropriate selection of microwave applicator is a crucial step and it depends upon the tumour structure, geometry and location as well as characteristics of the applicator such as its size, shape and its operating frequency [9]. Since the lossy nature of tissue effects antenna performance [10], the antenna has to be placed little far from the human body so that tissue properties do not change the antenna parameters and hence avoiding detuning the operating frequency. Also, the antenna has to be near the body for maximum power dissipation. Thus for minimizing mismatch losses and distance related losses an applicator is needed which couples appropriate power into the media by transferring of heat into the affected area only and leaving all the vicinity of it unaffected. Graphene-based patch applicator is therefore proposed here which may improve the efficacy of microwave hyperthermia treatment.

Besides the fact that graphene act as moderate conductor at microwave frequencies, the tunability property of graphene utilizing changing external bias helps in improving the conductivity of graphene [11-12]. Exclusive properties of graphene make it attractive for biomedical applications finds widespread use in drug delivery and photothermal therapy [13]. However, the use of graphene nanomaterial for microwave hyperthermia is still under trials. In this work, graphene-based microstrip patch antenna applicator has been proposed for the treatment of cancerous tumours with local control of the near-field heating pattern by shape, size, and feeding versatility [14].

Four different designs including rectangular, triangular, circular-shaped and ring-shaped double-slot in graphene patch antenna have been presented here. The proposed designs mounted on tri-layer human phantom have been investigated for optimally positioned distance from the body to obtain more localized heating and SAR distribution. The finite

element method (FEM) is used for implementation and analysis of the applicator designs in COMSOL Multiphysics software.

2. Materials And Methods

A. Design requirements

In this work, the basic geometries used for designing graphene patch antenna based on rectangular, circular, triangular and double-slot shapes are modelled considering the zig-zag arrangement of basic graphene structure [21]. Fig.1 depicts all the designs of graphene-based patch applicator. FR4 substrate having a dielectric constant of 4.5 is chosen for the antenna design since it is widely used for frequencies less than 1 GHz because the losses and absolute dielectric values are less critical in this range [15]. Microstrip line inset feeding of calculated dimensions is utilized with 50Ω impedance to match the load providing planar structure to the antenna. The graphene patch antenna is simulated to resonate at a frequency of 915 MHz using proper dimensions of the patch. The substrate of dimensions 110110 mm^2 is used for all the designs of the antenna. A 2-D monoatomic thin graphene layer is taken as a conducting patch having length L_p and width W_p.

The properties of graphene patch are assigned using material boundary conditions in COMSOL Multiphysics software. The design parameters are evaluated for various shapes of patch antenna from the equations given in [16] as listed in Table 1.

Table 1. Graphene patch antenna design parameters

Parameter	Design values
Length of the substrate, L_s	90 mm
Width of the substrate, W_s	70 mm
The thickness of the substrate, h	3 mm
The relative permittivity of a dielectric substrate, ε_r	4.5
Length of the rectangular patch, L_p	67 mm
Width of the rectangular patch, W_p	49 mm
Resonant frequency, f	915 MHz
The side length of the equilateral triangle patch, a	47.08 mm
The effective radius of a circular patch, r	48 mm
The effective radius of annular ring double slot patch, r_d	9 mm
Distance between two annular rings, d	4 mm
Length of feed, L_f	30.5 mm
Width of feed, W_f	4 mm

B. Graphene nanomaterial for applicator design

For using graphene as the radiator in the microwave regime, the patch of highly doped graphene having relaxation time of τ = 0.5ps and chemical potential μc = 0.25eV is utilized. The surface impedance of graphene defined as $Z_s = 1/\sigma_{graphene}$ can be reduced by changing the electrostatic bias voltage as it is reciprocal of conductivity which is given by Kubo's formula [17]. It consists of interband contribution and intraband contribution, while for microwave frequencies, the intraband contribution is mostly dominating whose formula is given in equation 1, where the interband contribution is negligible.

$$\underbrace{\sigma(\omega)}_{intraband} = \frac{2e^2 k_B T}{\pi \hbar^2} ln\left[2cosh\left[\frac{\mu_c}{2k_B T}\right]\right] \frac{j}{\omega + j\tau^{-1}} \quad \ldots\ldots\ldots\ldots\ldots\ldots\ldots\ldots\ldots\ldots\ldots\ldots\ldots\ldots(1)$$

where τ is the relaxation time, μ_c is the chemical potential, k_B is the Boltzmann's constant, h is the reduced Planck's constant i.e , T=h/2π is room temperature in Kelvins, ω is the radian frequency and e is the charge of an electron. Drude's Lorentz model is very closed-form representation for numerical simulation of the equation for conductivity if the condition $\mu_c >> h\omega$ is satisfied. The graphene patch antenna applicator is hence modelled using the electrical and non-electrical properties of graphene. The appropriate selection of properties of graphene material and chemical potential value enforces the graphene-based antenna to perform as a moderate conductor at microwave frequencies. The impedance could be further varied by application of gate potential to minimize distance related losses and mismatch losses.

C. Numerical modelling with human phantom

A four-layer human phantom model in a cylindrical shape is designed whose properties at 915 MHz. The phantom is having four layers of skin, fat, muscle and bone with a maximum radius of 100 mm for the outermost layer. The 4-layer human body phantom model is placed with the proposed antenna designs of different configurations at different positions. A 3-D numerical model of the graphene patch antenna and the human body was modelled and simulated for evaluating the temperature distribution in human organic tissue. The FEM based computation model for coupled EM and the thermal problem is given by the solution of the Maxwell equation and bioheat transfer equation (BHE) [18-19] respectively. The entire model is placed in a perfectly matched layer (PML) of radius 300 mm and a layer thickness of 50 mm to absorb outward going EM radiation from the computational model. The dielectric properties of the human tissue directly taken from reference [20] at 915 MHz are given in Table 2.

Table 2. Dielectric properties of human tissues

Tissue	Relative Permittivity (μ_r)	Relative Permeability (ε_r)	Conductivity (σ) [S/m]	Density (ρ) [kg/m^3]	Specific heat (C_p) [J/kg-K]	Thermal Conductivity (k) [W/m-K]
Skin	1	37	0.70	1100	3400	0.30
Fat	1	14.6	0.33	920	2500	0.25
Muscle	1	61	1.31	1041	3500	0.50
Bone	1	22.5	0.17	1500	1300	0.40
Tumour	1	59	0.65	1050	3639	0.50

COMSOL modelling of whole geometry for different shapes of patch antenna with 4-layer human body phantom is shown in Fig.2. In order to predict the induced fields into the target issues for coupled EM problems, the numerical

simulation of the bio-electromagnetic problem is done in RF module and heat transfer module of COMSOL using Multiphysics capability of the software to solve coupled problems.

3. Results And Discussion

The optimized design of four different configurations of graphene patch antenna applicators antenna at 915 MHz frequency for hyperthermia applications is used to obtain antenna performance parameters such as radiation pattern, polar plot gain and return loss parameters. Surface impedance of graphene is taking into consideration keeping in view that the maximum energy deposition is in the affected area, leaving all other healthy tissue areas in the vicinity. Though graphene is a moderate conductor at microwaves or mm waves, by varying the chemical potential, the conductivity of graphene can be enhanced so that the value of surface impedance gets lowered which is reciprocal of conductivity. The chemical potential is therefore set to 0.25 eV for all the configurations of graphene patch applicator. The formulation of the coupled problem of the human body phantom with the electromagnetic field is performed on COMSOL Multiphysics software using RF and heat transfer modules. The designed models are further analyzed using adaptive mesh refinement strategies.

Fig.3 shows the 3D graph of the radiation pattern of all the four shapes of graphene patch applicators. A far-field gain of 3.9 dBi, 4.3 dBi, 6.1 dBi and 5.9 dBi for rectangular, circular, triangular and double slot graphene patch applicator has been obtained respectively. It is observed that maximum gain is achieved at the top and more directives towards the body phantom.

Polar plot gain curves for the applicators are also shown in Fig.4. The plots are analysed in terms of far-field norm expressed by V/m. From all the simulation results of antenna performance characteristics, it has been observed that triangular patch antenna achieves a maximum gain of 6.1 dBi. Hence it is observed that it is the most preferred shape.

For satisfying the condition of impedance matching, return loss plot of four different shapes of patch applicator is shown in Fig.5. The maximum peak of -20.2 dB is achieved at 915 MHz frequency for triangular patch applicator which is observed as lower resonance peak among all the other applicators designs. These results suggested that the graphene patch applicators are designed at ISM band of 915 MHz for biomedical applications which are further used for the analysis of SAR and temperature distribution plots on human body phantom.

Further, the numerical results are presented in terms of SAR distribution and temperature distribution for different positions of the antenna.SAR distribution plots discussed in this section show that maximum SAR is obtained in the tumorous cells and surface currents are lowered in healthy tissues. For the minimization of distance-related losses and mismatch losses, the distance of patch from the body phantom is varied to find the optimized distance for obtaining a localized pattern of SAR. The performance is evaluated for distance variations from 0 to 20 mm with a step size of 3 mm. The curves for SAR and temperature distribution are demonstrated in Fig.6 and Fig.7 respectively as the distance is varied from 0 to 20 mm.

From the Table 3, it can be observed that patch applicators placed at an optimum distance of 3 mm result in the highest value of temperature as 320.3°K and SAR of 60.4 W/Kg for the rectangular applicator, 318.3°K and SAR of 54.7 W/Kg for circular patch applicator, 315.2°K and SAR of 54.2 W/Kg for double slot applicator and 324.3°K and SAR of 134.1 W/Kg for the triangular applicator.

The surface plots of temperature for different shapes of graphene-based patch applicator by modelling the geometry in the 3-D domain are shown in Fig.8 and it can be observed that triangular patch applicator obtains a maximum temperature of 324.3°K. Although double slot microstrip patch applicator also shows promising results for more

uniform heating of cylindrical tissues the triangular patch applicator has obtained higher value of SAR to destroy the unhealthy tissues as compared to double slot patch applicator.

Further analysis is performed to study the effect of heating inside the muscle phantom by examining the SAR and temperature distribution plots with respect to insertion depth inside the muscle phantom at an optimized distance of 3 mm as depicted in Fig.9 and Fig.10 respectively.

Table 3. SAR and temperature distribution values for a varying distance of patch applicator

The distance of patch applicator	Rectangular patch applicator		Circular patch applicator		Triangular patch applicator		Double slot patch applicator	
	SAR (W/kg)	Temperature (°K)	SAR (W/kg)	Temperature (°K)	SAR (W/kg)	Temperature (°K)	SAR (W/kg)	Temperature (°K)
0 mm	21.3	313.7	20.6	310.0	28.9	313.8	6.	310.6
3 mm	60.4	320.3	54.7	318.3	134.1	324.3	54.2	315.2
6 mm	48.5	318.9	44.6	316.8	88.2	319.0	47.5	312.5
9 mm	42.6	314.2	40.7	315.2	59.1	316.9	20.3	311.4
12 mm	30	313.7	28.6	314.1	41.5	313.7	10.1	310.8
15 mm	17	312.4	18.7	313.1	30.4	312.0	6.4	310.5
18 mm	6	310	5.0	312.5	10.8	311.4	3.7	310.20

The SAR distribution plots seemingly demonstrate highly localized heating for both triangular slot and double slot applicators. However, the heating patterns of conventional rectangular patch applicator and circular patch applicator show some dominant value of SAR and temperature distribution at other insertion depths also. Triangular patch applicator has maximum SAR of 124.3 W/kg and temperature of 323.9°K at insertion depth of 6 mm, double slot patch applicator has maximum SAR value of 49 W/kg and temperature of 316°K at insertion depth of 6 mm, circular patch applicator has maximum SAR of 57 W/kg and temperature of 315°K at insertion depth of 5 mm and rectangular patch applicator has maximum SAR of 73 W/kg and temperature of 319°K at insertion depth of 5 mm.

Table 4 compares SAR and temperature values for the proposed shapes of graphene patch applicators at different insertion depths considering the optimized distance of 3 mm and as expected the triangular patch applicator achieves maximum SAR value.

Table 4. SAR and temperature values at a different insertion depth

Insertion depth	Rectangular patch applicator		Circular patch applicator		Triangular patch applicator		Double slot patch applicator	
	SAR (W/kg)	Temperature (°K)	SAR (W/kg)	Temperature (°K)	SAR (W/kg)	Temperature (°K)	SAR (W/kg)	Temperature (°K)
0 mm	0.26	310.2	0.53	310.2	0.33	310.04	0.01	310.05
2 mm	15.5	311.8	7.08	310.9	3.5	310.2	4.2	310.44
4 mm	48.03	316.22	31.4	313.9	20.6	312.6	9.8	312.4
6 mm	23.23	314.9	21.53	314.7	124.3	323.9	41	315.9
8 mm	10.73	312.7	5.2	310.9	10.1	311.1	4.11	310.4
10 mm	1.69	310.4	3.9	310.3	3.6	310.6	1.11	310.02
0 mm	0.26	310.2	0.53	310.2	0.33	310.04	0.01	310.05

The results obtained from the designed antenna for four different shapes of patch applicator depicted in Table 3 and 4 can be used as a comparative measure for optimally selecting the graphene-based triangular patch applicator based on more localized heating patterns. The possibility of improved performance in triangular patch applicator can be owing to the zigzag arrangement at the edges of graphene patch as reported in [21]. The zigzag structure possesses higher input impedances which could cause effective suppression of surface currents for reduced backward heating. Further, the triangular shape has favourable features of compact design, low profile and occupies the lesser area.

4. Conclusions

The work presented here proposes different configurations for graphene-based antenna patch applicators which could provide a substantial improvement in uniform heating problem for non-invasive hyperthermia cancer treatment. The 3-D computational models are simulated using COMSOL software. The performance parameters of the antenna are evaluated for proper selection of antenna design parameters. SAR and temperature distribution results in human phantom demonstrate enhanced performance in case of graphene-based triangular patch applicator giving more localized heating than all the other shapes. The distance of patch applicator from human body phantom is varied for obtaining optimized distance and analysed that temperature and SAR values for triangular patch applicator are 324.3°K and 134.1 W/Kg respectively at 3 mm optimized distance. The results are also analysed for varied insertion depth within human phantom and it has been concluded that more localized superficial tumours are destroyed with the higher temperature at insertion depth of 6 mm.

Declarations

ACKNOWLEDGMENT

This work is supported by the DST FIST-2018 Project (Reference No. SR/ET-I/2018/157).

References

1. Y. Cheung and A. Neyzari, “Deep local hyperthermia for cancer therapy: external electromagnetic and ultrasound techniques,” *Cancer Research*, vol. 44, no. 10, pp. 4736–4744, 1984.
2. Sethi and S. K. Chakravarti, “Hyperthermia techniques for cancer treatment: A review,” *International Journal of PharmTech Research*, vol. 8, no. 6, pp. 292–299, 2015.

3. Raganella, G. Banci, I. Vannucci, C. Franconi, and C. A. Tiberio, “27 MHz conformal capacitive ring (CR) applicators for uniform hyperthermic/diathermic treatment of body segments with axial fields,” *IEEE Transactions on Biomedical Engineering*, vol. 36, no. 11, pp. 1124–1132, 1989.
4. B. Anderson, A. Baun, K. Harmark, L. Heinzl, P. Raskmark, and J. Overgaard, “A Hyperthermia system using a new type of inductive applicator,” *IEEE Transactions on Biomedical Engineering*, vol. BME-31, no. 1, pp. 21–27, 1984.
5. Tanabe, A. Mceuen, C. S. Norris, P. Fessenden, and T. V. Samulski, “A multi-element microstrip antenna for local hyperthermia,” *IEEE MTT-S International Microwave Symposium Digest*, pp. 183–185, 1983.
6. R. Stauffer, P. Maccarini, K. Arunachalam, O. Craciunescu, C. Diederich, T. Juang, F. Rossetto, J. Schlorff, A. Milligan, J. Hsu, P. Sneed, and Z. Vujaskovic, “Conformal microwave array (CMA) applicators for hyperthermia of diffuse chest wall recurrence,” *International Journal of Hyperthermia*, vol. 26, no. 7, pp.686–698, 2010.
7. S. Ebbini, S. I. Umemura, M. Ibbini, and C. A. Cain, “A cylindrical-section ultrasound phased-array applicator for hyperthermia cancer therapy,” *IEEE Transactions on Ultrasonics, Ferroelectrics, and Frequency Control*, vol. 35, no. 5, pp. 561–572, 1988.
8. Montecchia, “Microstrip-antenna design for hyperthermia treatment of superficial tumors,” *IEEE Transactions on Biomedical Engineering*, vol. 39, no. 6, pp. 580–588, 1992.
9. P. Singh, “Microwave applicators for hyperthermia treatment of cancer: An overview,” *3rd International Conference on Microwave and Photonics (ICMAP)*, pp. 1–3, 2018.
10. H. A. Rahman, Y. Yamada, M. S. A. Nordin, “Analysis on the effects of the human body on the performance of electro- textile antennas for wearable monitoring and tracking application,” *Materials*, vol. 12, no. 10, pp. 1636–1636, 2019.
11. B. Lu, H. Chen, and Z. G. Liu, “A review of microwave devices based on CVD-grown graphene with experimental demonstration,” *EPJ Applied Metamaterials*, vol. 6, pp. 8–8, 2019.
12. Mencarelli, M. Dragoman, L. Pierantoni, T. Rozzi, and F. Coccetti, “Design of a coplanar graphene-based nano-patch antenna for microwave application,” *2013 IEEE MTT-S International Microwave Symposium Digest (MTT)*, pp. 1–4, 2013.
13. Yang, A. M. Asiri, Z. Tang, D. Du, and Y. Lin, “Graphene based materials for biomedical applications,” *Materials Today*, vol. 16, no. 10, pp. 365–373, 2013.
14. Bala, R. Singh, A. Marwaha, and S. Marwaha, “Wearable graphene based curved patch antenna for medical telemetry applications” *Applied Computational Electromagnetics Society Journal*, no. 5, pp. 31–31, 2016.
15. R. Aguilar, M. Beadle, P. T. Thompson, and M. W. Shelley, “The microwave and RF characteristics of FR4 substrates”.
16. Kiruthika and T. Shanmuganantham, “Comparison of different shapes in microstrip patch antenna for X-band applications,” *2016 International Conference on Emerging Technological Trends (ICETT)*, pp. 1–6, 2016.
17. Bozzi, L. Pierantoni, and S. Bellucci, “Applications of Graphene at Microwave Frequencies,” pp. 661–669, 2015.
18. C. Shih, P. Yuan, W. L. Lin, and H. S. Kou, “Analytical analysis of the Pennesbioheat transfer equation with sinusoidal heat flux condition on skin surface,” *Medical Engineering & Physics*, vol. 29, no. 9, pp. 946–953, 2007.
19. Weinbaum and L. M. Jiji, “A New Simplified Bioheat Equation for the Effect of Blood Flow on Local Average Tissue Temperature,” *Journal of Biomechanical Engineering*, vol. 107, no. 2, pp. 131– 139, 1985.
20. Gabriel, R. W. Lau, and C. Gabriel, “The dielectric properties of biological tissues: III. Parametric models for the dielectric spectrum of tissues,” *Physics in Medicine and Biology*, vol. 41, no. 11, pp. 2271– 2293, 1996.
21. Bala, A. Marwaha, S. Marwaha, “Comparative analysis of zigzag and armchair structures for graphene patch antenna in THz band” *Journal of Material Science Electronics Letters,* vol. 27 no. 5, pp. 5064–5069, 2016.

Figures

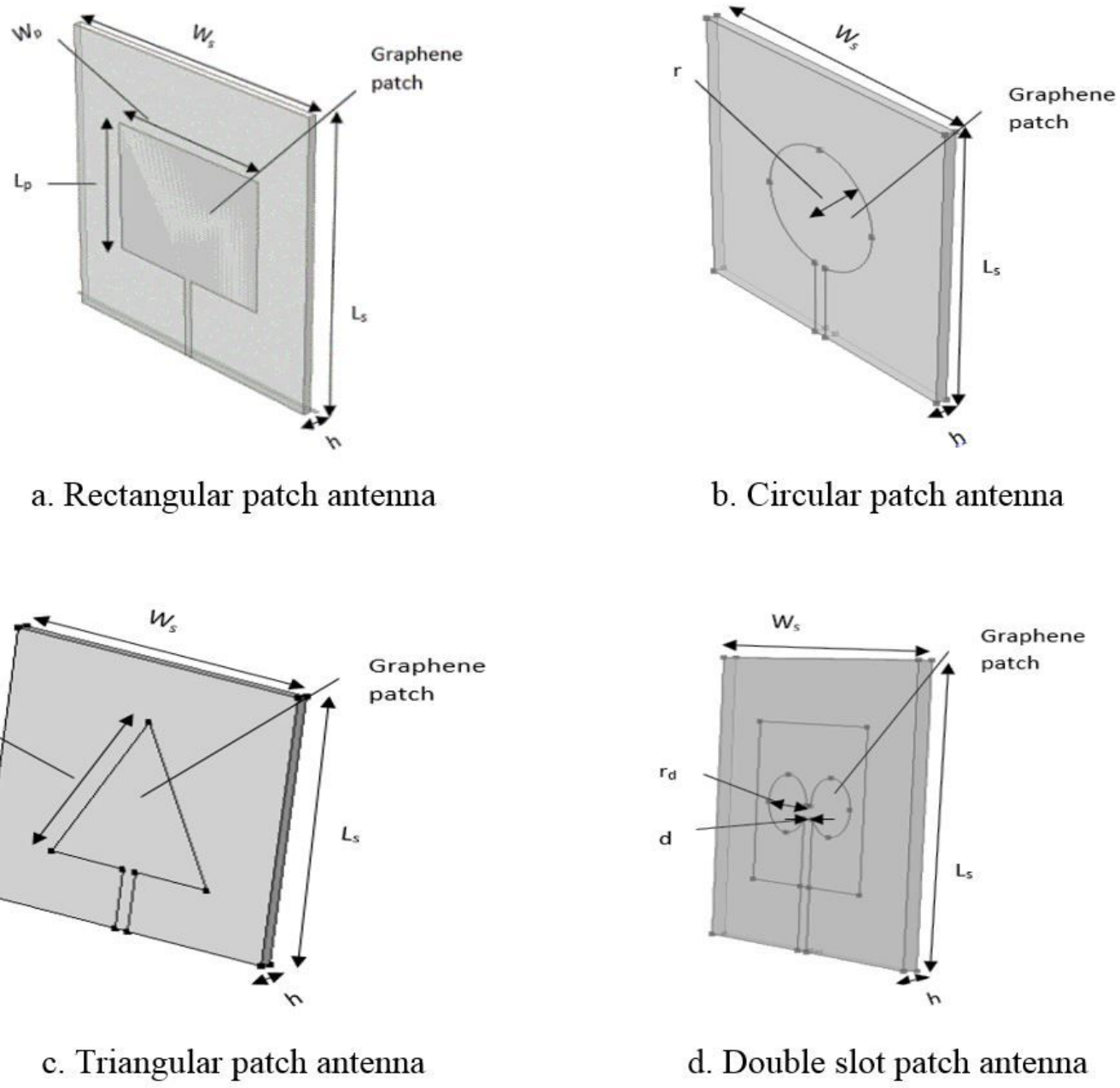

Figure 1

Different shapes of the graphene-based patch antenna

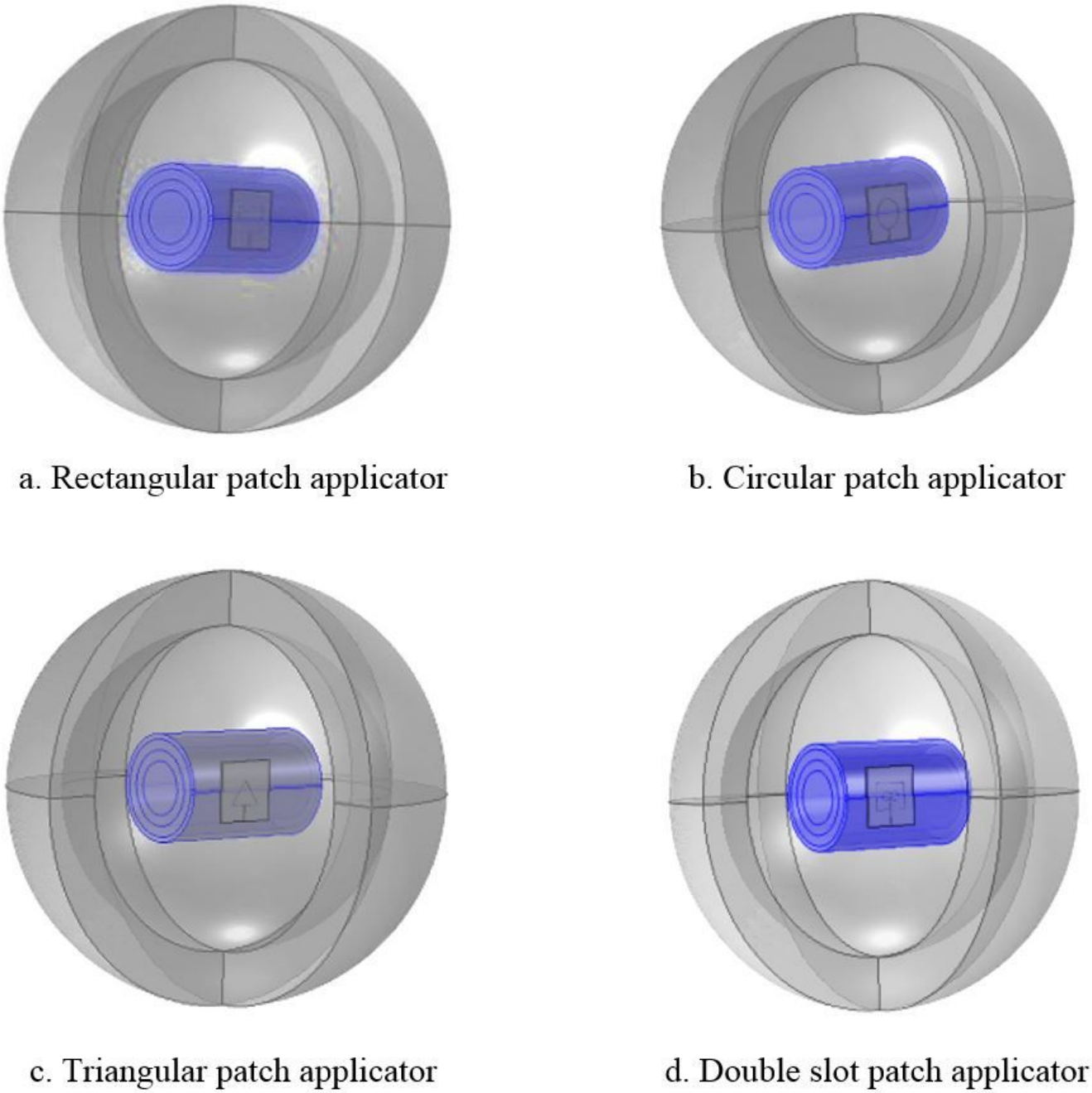

Figure 2

Patch applicator models with body phantom

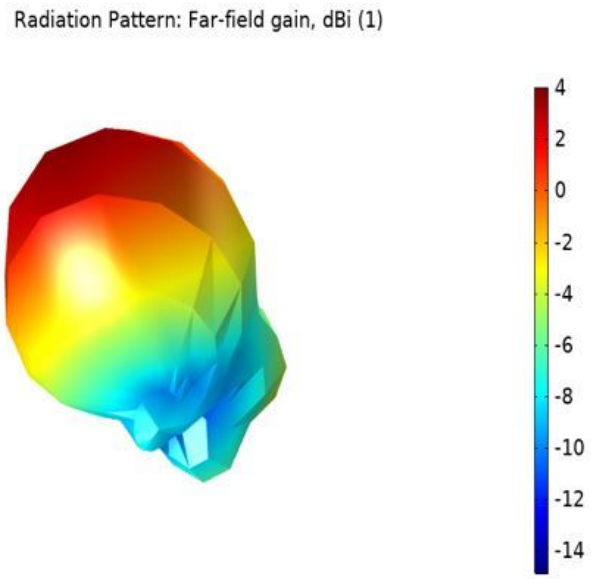

a. Rectangular patch applicator

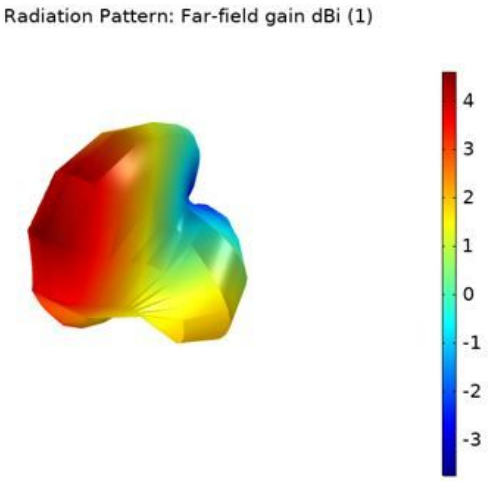

b. Circular patch applicator

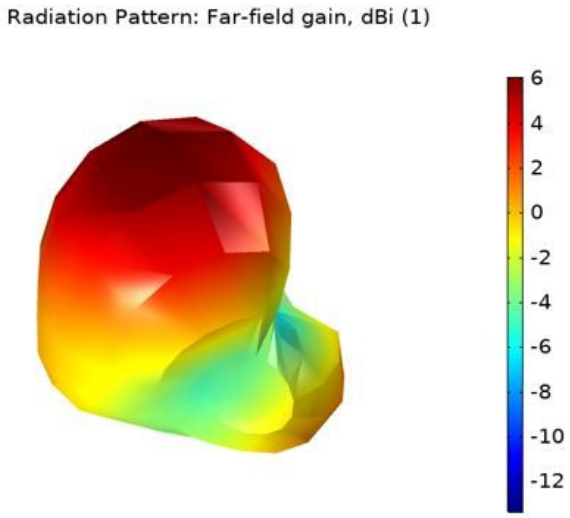

c. Triangular patch applicator

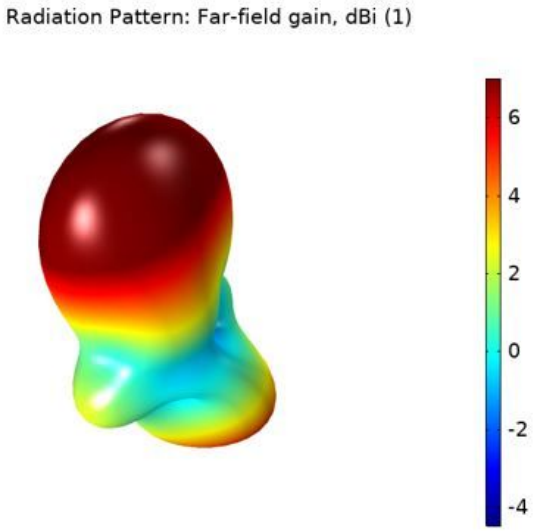

d. Double slot patch applicator

Figure 3

Radiation pattern plots

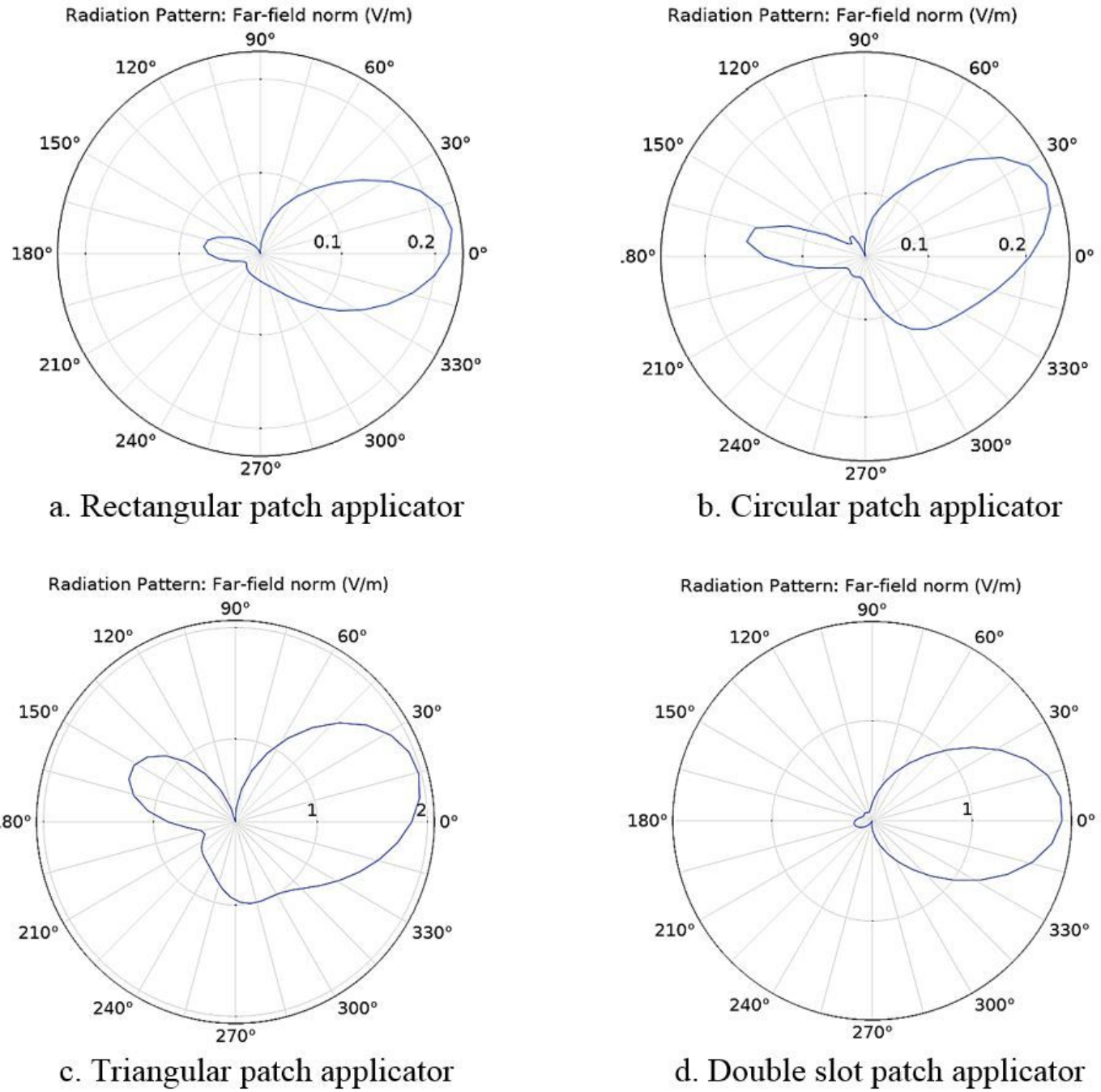

Figure 4

Polar plot gain graph

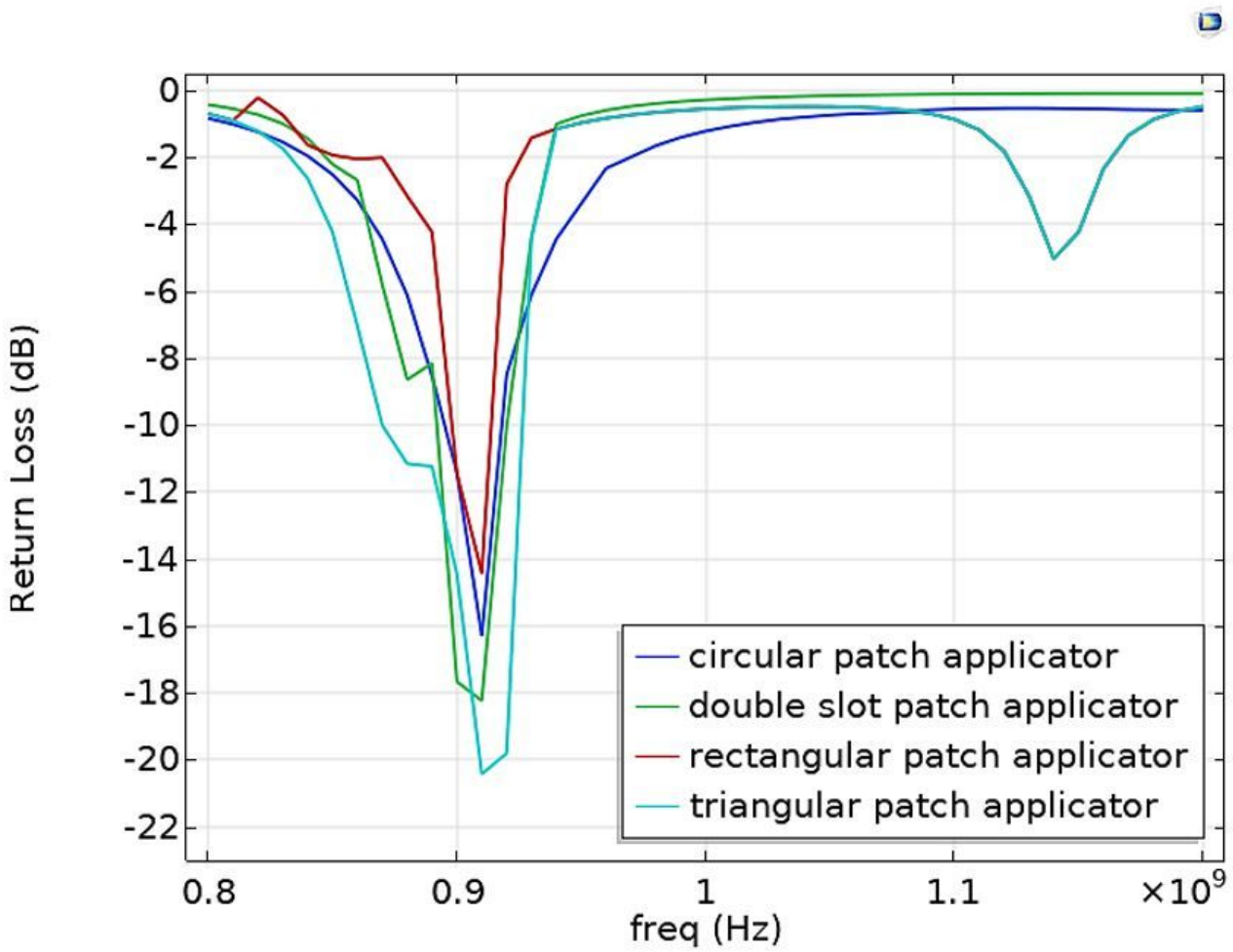

Figure 5

Return loss plot for different graphene patch applicators

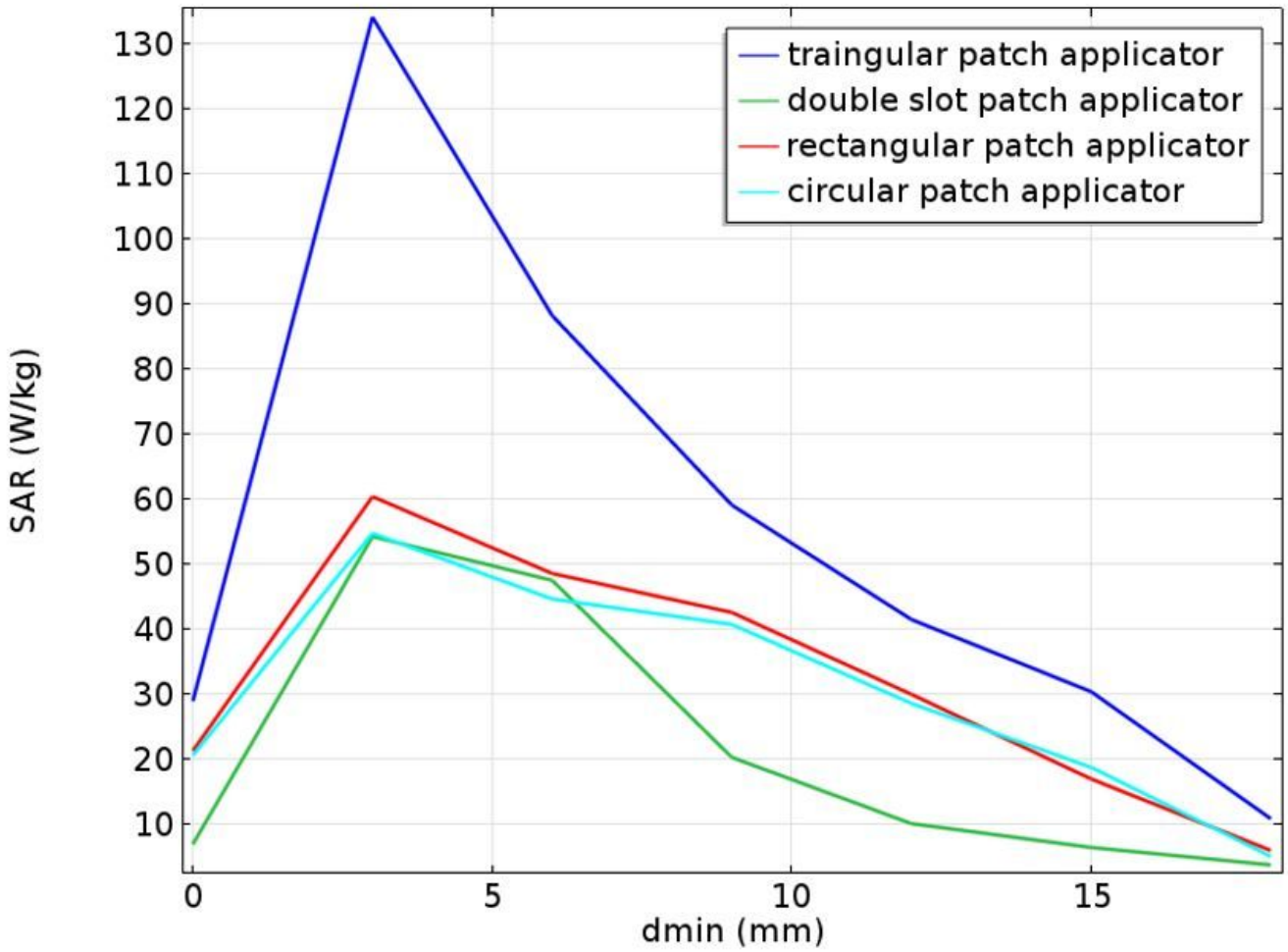

Figure 6

SAR versus optimized distance plot

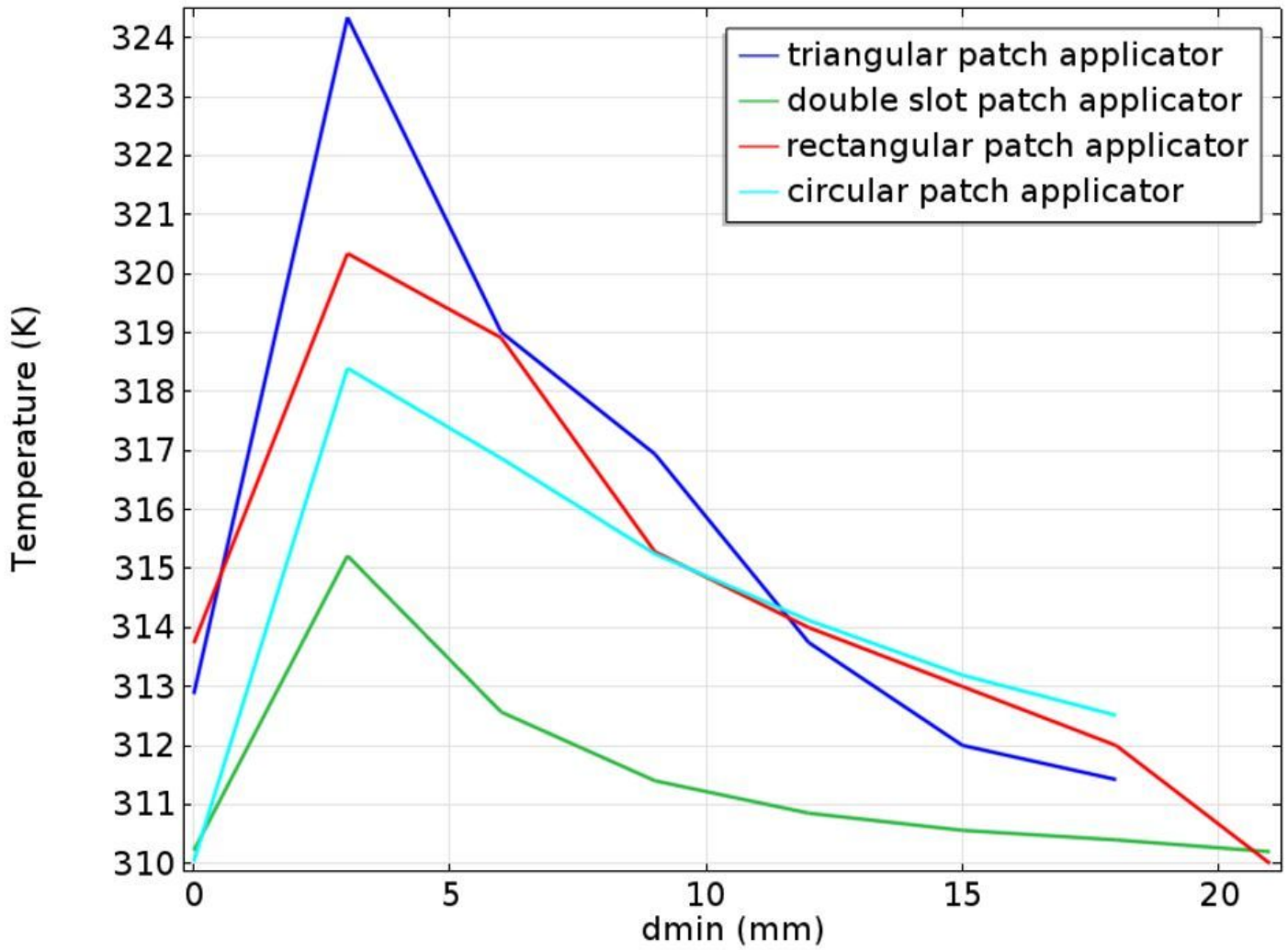

Figure 7

Temperature distribution versus optimized distance plot

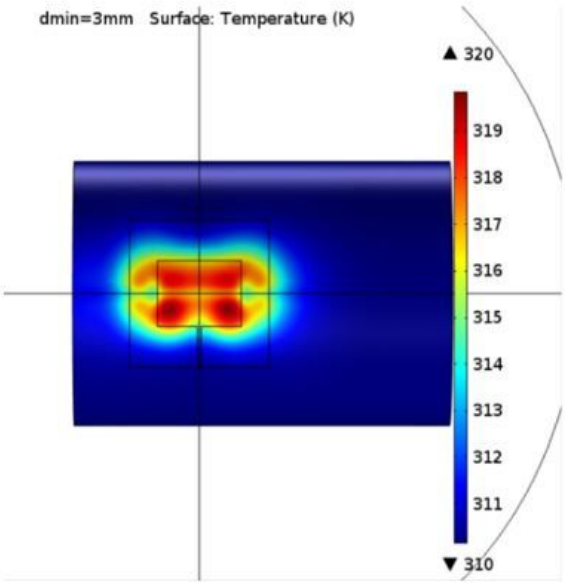

a. Rectangular patch applicator

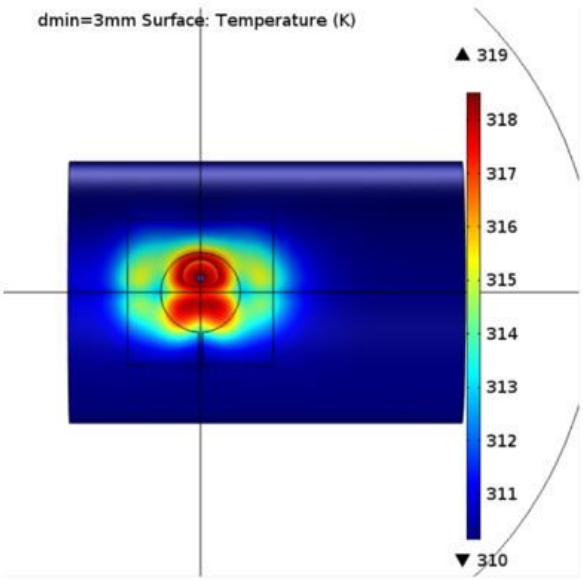

b. Circular patch applicator

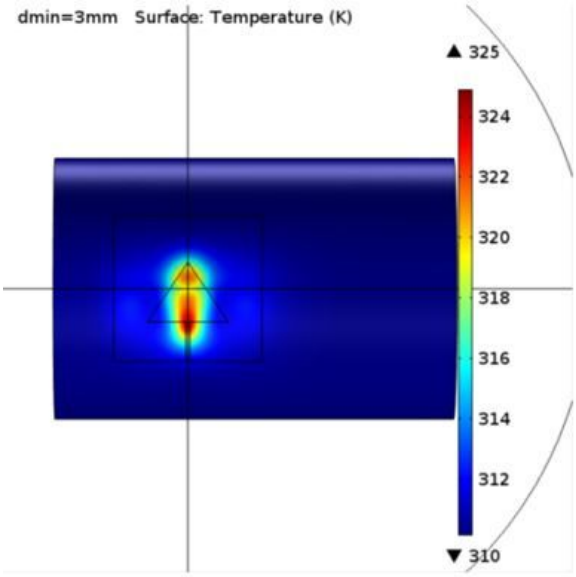

c. Triangular patch applicator

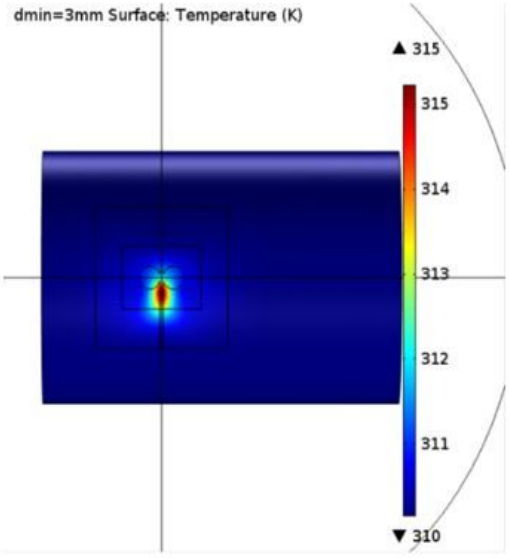

d. Double slot patch applicator

Figure 8

Surface plots for temperature distribution

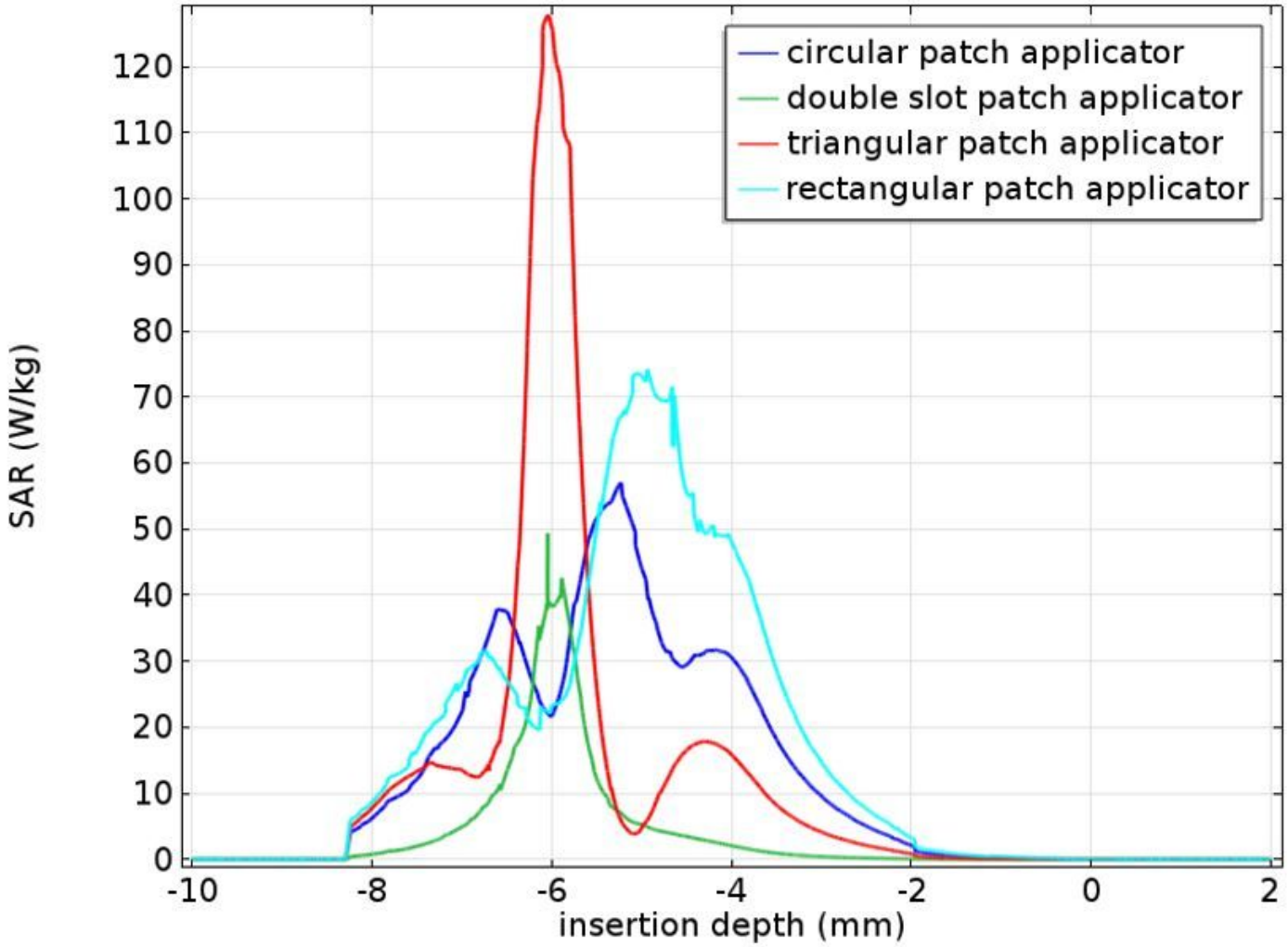

Figure 9

SAR versus insertion depth plot

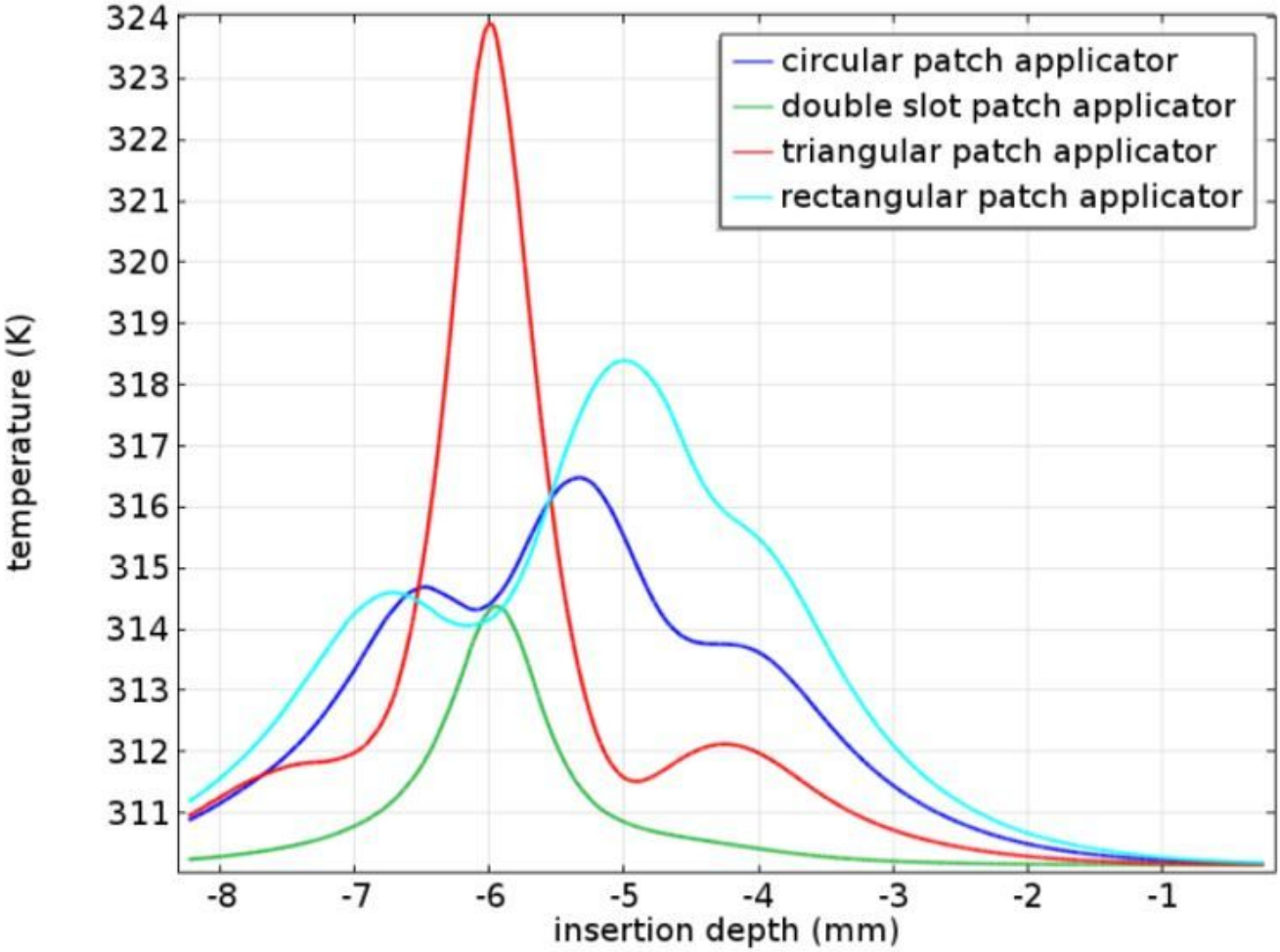

Figure 10

Temperature distribution versus insertion depth plot